

# CAUSES OF THE OCCURRENCE OF AN "EFFECTIVE" POROSITY IN GRANULAR MEDIA

V. A. Nelidov

UDC 532.546

The cause of the difference between the total  $\varepsilon$  (geometric) and "effective"  $\varepsilon_{\text{ef}}$  (hydrodynamic) porosity of granular media is established.

One of the unsolved problems in the investigation of the hydrodynamics of granular media is the evaluation of the participation of the volume of the intergranular void  $V_v$  in the investigated process. The majority of investigators presume that all its elements participate equally in the percolation process and in hydrodynamic calculations take the entire magnitude of the intergranular porosity of the layer

$$\varepsilon = V_v/V_l. \quad (1)$$

In the opinion of others [1-5] it is necessary to take account of the effectiveness of the participation of the intergranular volume in percolation, in connection with which  $V_{\text{ef},v}$  should be less than  $V_v$  and in calculations it is necessary to use the quantity

$$\varepsilon_{\text{ef}} = V_{\text{ef},v}/V_l. \quad (2)$$

The existence in the intergranular void of stagnant zones not participating in percolation is the most frequent suggestion to account for the occurrence of  $\varepsilon_{\text{ef}}$ . However, to date this assumption has been open to dispute owing to the lack of convincing experimental data allowing the magnitude of this effect to be judged. In our opinion, the possibility of its existence can be verified indirectly by comparing the percolation conditions in a granular medium with fluid flow through a capillary having a spherical enlargement where stagnation is observed. For this purpose we investigated four capillaries of the same length ( $L=100$  mm) and diameter ( $d=1.43$  mm). Three capillaries had a spherical enlargement in the middle of diameter  $D_3=6$ ,  $D_2=9$ , and  $D_1=12.7$  mm, respectively. Stagnation of water in the spherical enlargements was confirmed by direct visual observation: they were first filled with transparent water and then a colored flow was passed through the capillary; within a certain time period this flow penetrated the spherical enlargement as a colored "rod," the unaffected transparent water remaining around the periphery. A characteristic feature of fluid flow in such capillaries is the unusual type of graphical dependence  $Q=f(\Delta p)$ , which in the laminar flow region is expressed not by sloping straight lines but in the form of curves, as shown in Fig. 1. We see from Fig. 1 that the curves in the region of small  $\Delta p$  have rectilinear branches located above the sloping straight line for the fourth capillary, which does not have a spherical enlargement. On increase in  $\Delta p$  the lines change into curves toward the side opposite to the effect of the turbulent (inertial) forces. The larger the spherical enlargement, the greater the deviation of the curve from the rectilinear branch. These curves were obtained in an investigation of a Newtonian fluid - oil with a viscosity of  $1.9659 \text{ N}\cdot\text{sec}/\text{m}^2$  ( $t=20^\circ\text{C}$ ); the investigated capillaries were substituted for the usual capillaries in a constant flow-rate capillary viscosimeter [6].

The increase of the throughput of the enlarged capillaries (curves 1-3) in the region of small  $\Delta p$  (in comparison with the throughput of the unenlarged capillary 4 for the same  $\Delta p$ ) can be explained by the lack of adhesion of the fluid to the capillary walls when the fluid "rod" is passing through the spherical enlargement. The deviation from the straight lines graphically depicting the dependence  $Q=f(\Delta p)$  for inflated capillaries apparently arises because the cross section of the fluid "rod" begins to expand as it enters the spherical enlargement; this effect becomes apparent only at appreciable  $\Delta p$ .

---

Translated from *Inzhenerno-Fizicheskii Zhurnal*, Vol. 21, No. 6, pp. 1017-1024, December, 1971.  
Original article submitted March 2, 1971.

© 1974 Consultants Bureau, a division of Plenum Publishing Corporation, 227 West 17th Street, New York, N. Y. 10011. No part of this publication may be reproduced, stored in a retrieval system, or transmitted, in any form or by any means, electronic, mechanical, photocopying, microfilming, recording or otherwise, without written permission of the publisher. A copy of this article is available from the publisher for \$15.00.

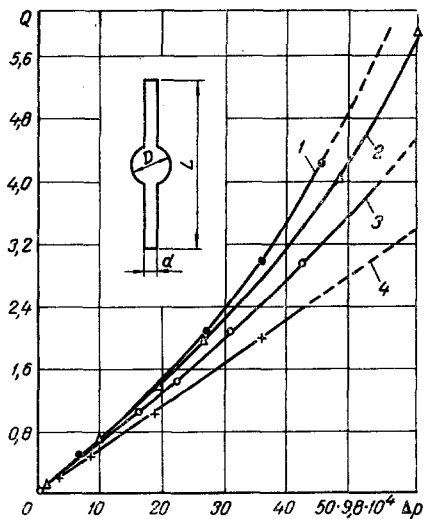


Fig. 1. Dependence  $Q = f(\Delta p)$  for fluid flow through the investigated capillaries ( $Q$ ,  $\text{cm}^3/\text{sec}$ ;  $\Delta p$ ,  $\text{N}/\text{m}^2$ ).

Thus, it follows from the experimental results that stagnation of the fluid in the channels can be detected by analyzing the graphical dependences  $Q = f(\Delta p)$  which, even before the transition to the turbulent region, should be characterized by a deviation from the straight lines toward an intensified increase of  $Q$  as  $\Delta p$  increases. However, no such deviations are found in investigations of the analogous dependence for granular media and, before the effect of inertial forces appears, the rectilinear Darcy's law holds. On the basis of this we can conclude that stagnant zones not participating in percolation do not exist in real granular media, although the intergranular volume is characterized by constrictions and enlargements. This is because the expansions in a granular medium communicate with one another in different directions by means of several narrow passages, so that the differently directed fluid threads involve practically the entire volume of the intergranular expansions in percolation even at small  $\Delta p$ . However, the equality  $\epsilon_{\text{ef}} = \epsilon$  still does not follow from this, since differences in the degree of effectiveness of the participation of wide and narrow pores in percolation can also lead to its disruption. Thus, the flow velocity in wide pores should be considerably less than the flow velocity in narrow pores. In connection with this, the participation of the volume of intergranular voids ac-

counted for by wide pores in percolation will be considerably less effective than the participation of voids accounted for by narrow pores. For a quantitative evaluation of the indicated effect we will consider the case of a steady flow around cylindrical obstacles having axes parallel to each other and perpendicular to the direction of the flow. This type of flow will be plane, which is convenient when examining the force pattern of penetration through a granular medium, and at the same time will be characterized by a variable cross section, as is observed in a real granular medium.

We will analyze two cases of the arrangement of the cylinders - hexagonal and square (Fig. 2); the hydraulic flow through them is taken to be potential (rotation of velocity is absent) and to be described by the Laplace equation. Then, in conformity with field theory and the theory of functions of a complex variable [7, 8], we can represent the structure of the flow by constructing streamlines and lines of equal potential (equipotential lines). On the basis of a formal mathematical analogy between the equations of hydro- and electrodynamics we can construct the same such net also for an electric current in a plane conducting medium. For the unit cells of the hexagonally arranged cylinders the nets were constructed by the graphical method [9]. For the square arrangement we constructed the nets experimentally by determining the equipotential lines of an electric field in an electrolytic cell by the electrolytic tank method [10]. For the hexagonal arrangement of the cylinders the unit cell will be a rectangle with sides  $a$  and  $L = a\sqrt{3}$ ; for the square arrangement it will be a square with side  $L$ . The nets obtained for these cells are shown in Fig. 3. As we see from Fig. 3, the curvilinear squares forming the net have different sizes, although the condition of their hydrodynamic equivalence was fulfilled in constructing them. In constricted sections the hydrodynamic squares are smaller in area than in enlarged sections, which is a clear reflection of the higher effectiveness of the participation in percolation of the constricted section as compared with the enlarged zone of the channel.

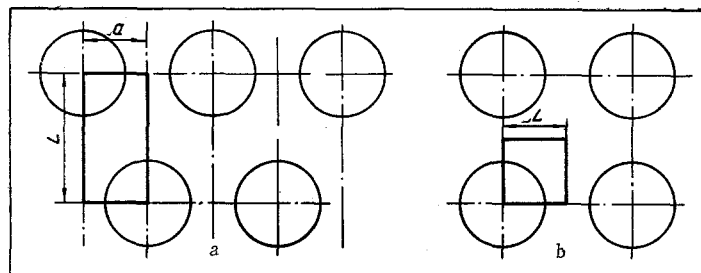


Fig. 2. Unit cells in the case of a hexagonal (a) and square (b) arrangement of the cylinders.

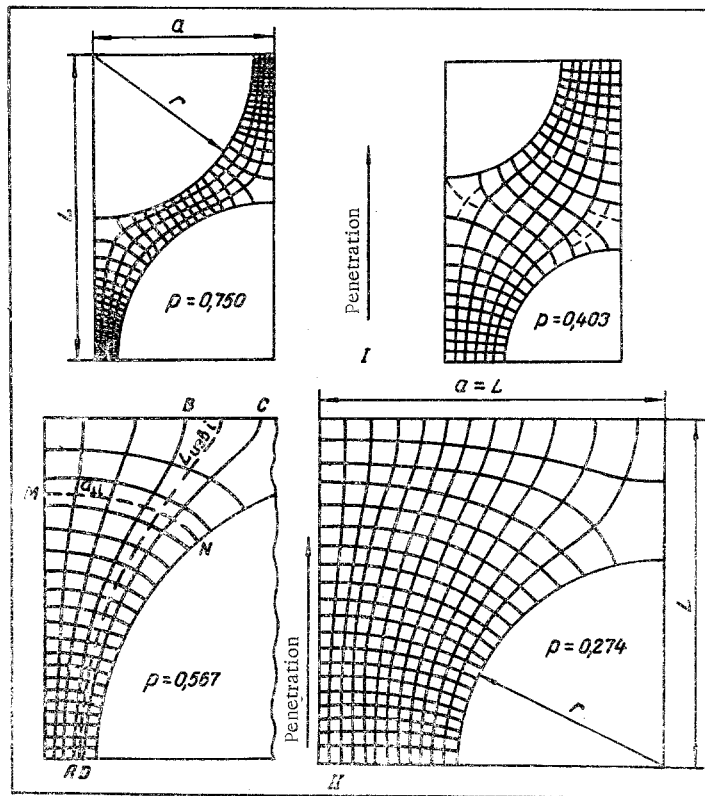


Fig. 3. Electric force field of unit cells for hexagonal (I) and square (II) arrangement of the cylinders.

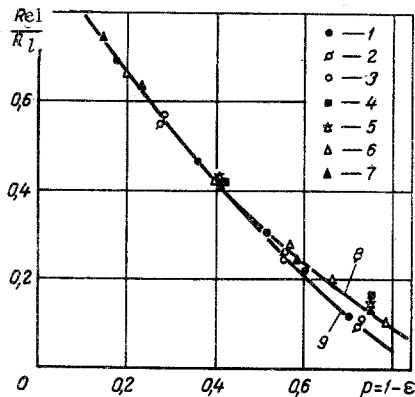


Fig. 4. Relative permittivity  $R_{el}/R_L$  of unit cells as a function of the packing density  $p = 1 - \epsilon$  of cylinders arranged as a square (1-3) and as a hexagon (4-7); 1) experiment; 2) calculated by Eq. (7a); 3, 4) by Eq. (6); 5) by Eq. (7); 6) experiment; 7) taken from [9]; 8) constructed according to [9]; 9) according to [8].

The greater the difference between the wide and narrow section, the more  $\epsilon_{ef}$  differs from  $\epsilon$ . Thus we can conclude that, when substituting porosity values into hydrodynamic equations, it is necessary to take into account the characteristics arising in the intergranular void during percolation: different elements of the intergranular void participate in percolation with a different effectiveness, and so it is necessary to substitute the quantity  $\epsilon_{ef}$  and not  $\epsilon$  into hydrodynamic equations. Hence it is reasonable to call the value of  $\epsilon_{ef}$  the hydrodynamic intergranular porosity and  $\epsilon$  the geometric intergranular porosity.

For a quantitative evaluation of the effect of constrictions and enlargements of the flow, we will determine its tortuosity from the tortuosity of unit tubes of force (of the type ABCD in Fig. 3) and the cross section normal to the tortuous flow from the length of the equipotential lines (of type MN in Fig. 3).

To determine the tortuosity of the flow, we measured at first the lengths  $L_{tor, i}$  of the axes of the unit tubes of force, the number of which was  $z$ . Then we calculated the arithmetic mean values of  $L_{tor}$  and the ratio  $L_{tor}/L$ . To determine the cross section of the flow normal to the tortuous tubes of force, we measured the extent of the equipotential lines, the number of which was  $w$ , and calculated the arithmetic mean length  $a_{\perp}$  and the ratio  $a_{\perp}/a$  (for unit cells of the square packing of the cylinders  $L = a$ ).

The ratios  $L_{tor}/L$  and  $a_{\perp}/a$  obtained thereby for each field (Fig. 3) are presented in Table 1. On the basis of these results we determined the values of  $\epsilon_{ef}$ , which for the two-dimensional problem can be calculated by the equation

$$\epsilon_{ef} = \frac{L_{tor}}{L} \cdot \frac{a_{\perp}}{a} \quad (3)$$

As we see from Table 1, in all investigated cases the values of  $\epsilon_{ef}$  were less than the values of  $\epsilon$  calculated by the usual method.

TABLE 1. Geometric and Hydrodynamic Characteristics of Packings of Cylindrical Bodies

Type of packing of cylinders	Hexagonal		Square		
	$\varepsilon$	0,597	0,250	0,720	0,433
$\frac{L_{\text{tor}}}{L}$	1,195	1,260	1,061	1,080	1,050
$\frac{a_{\perp}}{a}$	0,468	0,176	0,567	0,295	0,114
$\varepsilon_{\text{ef}}$	0,520	0,222	0,624	0,319	0,120
$\varepsilon_{\text{ef}}/\varepsilon$	0,870	0,890	0,860	0,736	0,440

In concluding our analysis of Fig. 3, we should note that when determining  $\varepsilon_{\text{ef}}$  from the force field it is desirable to have a "density" of the hydrodynamic net such that its further "compaction" would have practically no effect on the arithmetic mean values of  $a_{\perp}$  and  $L_{\text{tor}}$ . The fields presented in Fig. 3 do not claim to be such a case, although they are close to it. They serve primarily to illustrate convincingly the causes of the decrease of the hydrodynamic  $\varepsilon_{\text{ef}}$  with respect to the geometric  $\varepsilon$ .

We will verify the values of  $L_{\text{tor}}/L$ ,  $a_{\perp}/a$ , and  $\varepsilon_{\text{ef}}$  given in Table 1. For this purpose we represent the unit cells shown in Fig. 3 in the form of electrolytic tanks and fill them with electrolyte. We will express the electrical resistance  $R_l$  of the tanks in terms of the tortuous path of penetration  $L_{\text{tor}}$  and cross section normal to the tortuous flow  $a_{\perp}$ , assuming in so doing that the cylindrical inclusions are electrically nonconducting. This resistance is

$$R_l = \rho \frac{L_{\text{tor}}}{a_{\perp}}. \quad (4)$$

Without cylindrical inclusions these same tanks will have resistance

$$R_{\text{el}} = \rho \frac{L}{a}. \quad (5)$$

The relative permittivity of the cells will be equal to

$$\frac{R_{\text{el}}}{R_l} = \frac{La_{\perp}}{L_{\text{tor}}a}. \quad (6)$$

Then, substituting the values of Table 1 into (6) we can calculate the values of  $R_{\text{el}}/R_l$ . Now we compare them with the values which can be obtained also by calculation on the basis of the ratio of the number of tubes of force  $z$  to the number of equipotential lines  $w$ , as was done in [9]. For the hexagonal arrangement of the cylinders

$$\frac{R_{\text{el}}}{R_l} = \frac{z}{w} \sqrt{3}, \quad (7)$$

and for the square arrangement

$$R_{\text{el}}/R_l = z/w.$$

Moreover, for an additional comparison the ratios  $R_{\text{el}}/R_l$  were determined experimentally in electrolytic tanks duplicating the contours of the unit cells shown in Fig. 3. We measured  $R_{\text{el}}$  and  $R_l$  by means of an ac bridge at frequency 5000 Hz. Thus, for each  $\varepsilon$  of Table 1 we determined the values of  $R_{\text{el}}/R_l$  three times in a different way, which, in addition to a comparison with each other, were compared also with the experimental data obtained in [9] (in [9]  $K_r = R_{\text{el}}/R_l$ ) and were also checked by the analytic Rayleigh-Runge formula [11, 12] which has the form

$$\frac{R_{\text{el}}}{R_l} = 1 - \frac{2p}{1 + p - 0.306p^4 - 0.013p^8}, \quad (8)$$

where  $p = 1 - \varepsilon$ .

The results of determining  $R_{\text{el}}/R_l$  and their comparison with each other are presented in Fig. 4. We see from Fig. 4 that when  $p < 0.4$  the values of  $R_{\text{el}}/R_l$  both for the square and for the hexagonal arrangement of the cylinders are practically the same.

The results begin to diverge with an increase of  $p > 0.4$ . For the square packing the calculated (by Eqs. (6) and (7a)) and experimental points agree well with the Rayleigh-Runge formula. For the hexagonal arrangement of the cylinders the points obtained from Eqs. (6) and (7) and by experiment agree well with one another and with the experimental data [9]. They are located near a curve obeying the expression obtained on eliminating terms with higher powers of  $p$  from the Rayleigh-Runge formula, i.e.,

$$\frac{R_{el}}{R_l} = 1 - \frac{2p}{1+p} \quad (9)$$

Thus the data of Table 1 illustrating the inequality between  $\varepsilon$  and  $\varepsilon_{ef}$  are confirmed by several independent methods.

#### NOTATION

$V_l$	is the volume of the porous specimen (layer);
$V_v$	is the total volume of the intergranular voids of the porous specimen;
$\varepsilon_{ef,v}$	is the effective volume of the intergranular voids of the porous specimen;
$\varepsilon$	is the total intergranular porosity;
$\varepsilon = V_v/V_l$ ;	
$\varepsilon_{ef}$	is the effective intergranular porosity;
$\varepsilon_{ef} = V_{ef,v}/V_l$ ;	
$L$	is the length of the porous specimen or the unit cells along which penetration is directed;
$L_{tor}$	is the length of tortuous path of penetration in a unit cell or in a porous medium;
$L_{tor}/L$	is the tortuosity;
$a$	is the transverse dimension of the unit cell;
$a_{\perp}$	is the arithmetic mean length of equipotential lines in a unit cell;
$R_l$	is the electrical resistance of an electrically nonconducting porous specimen (layer) on filling its pores with electrolyte;
$R_{el}$	is the electrical resistance of the electrolyte poured into the tank from which the porous specimen has been removed;
$R_{el}/R_l$	is the relative permittivity of the porous specimen;
$\rho$	is the specific resistance of the electrolyte;
$\Delta p$	is the pressure drop.

#### LITERATURE CITED

1. Zigel', Percolation [in Russian], GONTI (1939).
2. S. Kiesskalt, *Chemie-Ing-Techn.*, No. 1, 14 (1954).
3. O. N. Grigorov, Z. P. Koz'mina, A. V. Markovich, and D. A. Fridrikhsberg, *Electrokinetic Properties of Capillary Systems* [in Russian], Izd. AN SSSR (1956).
4. L. E. Brownell, D. C. Gami, R. A. Miller, and W. E. Nekarvis, *AIChE*, 2, No. 1, 19 (1956).
5. B. F. Stepochkin, *Nauchnye Doklady Vyssh. Shkoly, Khimiya i Khim. Tekhnologiya*, No. 1, 210 (1959).
6. G. V. Vinogradov, V. A. Nelidov, N. G. Pavlov, and I. M. Sapozhnikov, Author's Certificate No. 210470 cl. 42, 7/01; *Byull. Izobr.*, No. 6 (1968).
7. A. D. Al'tshul' and P. G. Kiselev, *Hydraulics and Aerodynamics* [in Russian], Izd. Lit. po Stroitel'stvu (1965).
8. L. Prandtl and O. Tietjens, *Hydro- and Aeromechanics* [Russian translation], Vol. 1, Gos. Tekhn.-Teor. Izd. (1933).
9. V. P. Mashovets, *Zh. Prikl. Khim.*, 24, No. 4, 353 (1951).
10. N. P. Glukhanov, Ya. P. Kovalevskaya, K. I. Krylov, G. Ya. Murav'eva, and V. N. Rudakov, in: *Laboratory Studies of an Electromagnetic Field* [in Russian], LETI im. V. I. Ul'yanova (Lenina), Leningrad (1957).
11. Rayleigh, *Philos. Mag.*, Ser. 5, 34, 481 (1892).
12. Runge, *Z. Techn. Phys.*, No. 2, 61 (1925).